

## FINITE ELEMENT AND APPLIED MODELS OF THE STEM WITH SPIKE DEFORMATION

Besarion MESKHI<sup>1</sup>, Dmitry RUDOY<sup>1</sup>, Yuri LACHUGA<sup>2</sup>, Viktor PAKHOMOV<sup>1,3</sup>,  
Arkady SOLOVIEV<sup>1</sup>, Andrey MATROSOV<sup>1</sup>, Ivan PANFILOV<sup>1</sup>, Tatyana MALTSEVA<sup>1</sup>

<sup>1</sup>Don State Technical University, 1 Gagarin Sq., 344003 Rostov-on-Don, Russia

<sup>2</sup>Russian Academy of Sciences (RAS), 32 a Leninsky ave., 119334, Moscow, Russian Federation

<sup>3</sup>FSBSI Agricultural Research Center "Donskoy", 3 Nauchny Gorodok Street., 347740 Zernograd, Rostov Region, Russia

Corresponding author email: dmitriyrudoi@gmail.com

### Abstract

*Considered by this article are static and dynamic deformation of the stem with the ear of wheat and of the individual grain. The purpose of the article is to determine the factors of influence on the ear of wheat to isolate the grain. The ear fluctuations are considered within the Euler-Bernoulli bar theory. The first stage studies the dynamics of the plant as a whole, the second stage studies the dynamics of an individual grain in a moving system associated with the ear. The model of the ear and the grain fluctuation uses the mechanical characteristics of elastic bonds and elastic bodies, which are determined by spring stiffness's, elastic moduli, etc. The natural frequencies shows that at the value of natural frequencies of grain fluctuations 131,6 Hz and 1274,9 Hz the grain itself fluctuates predominantly, and at frequencies 1622,8 Hz, 7367.3 Hz, 9396.0 Hz and 13491,0 Hz the flakes vibrate.*

**Key words:** early stages of maturation, ear fluctuations, grain of wheat, harvest, mathematical model.

### INTRODUCTION

Agriculture was and is the most important sector of our country's national economy. Agribusiness must meet the growing needs, on the one hand, of the population for food, and, on the other hand, of the industry - for raw materials (Andruszczak P.K.S. et al., 2019; Berihuete-Azorin M. et al., 2020). Modern production implies a highly efficient use of the production potential of the agro-industrial complex; technical, quality and, especially, reliability upgrade of agricultural machinery; reducing losses and improving the quality of agricultural products.

Modern agriculture is unthinkable without the cultivation and production of grain crops. Grain crops occupy an area over 40 million hectares in the Russian Federation, which is 10% of the world's land area. Grain is the main and indispensable product in the human diet as well as productive farm animals and the main element of food security (Pakhomov V. et al., 2015; 2016; Rybas I. et al., 2016). Grain crops have high nutritional, taste and dietary properties. Grain production achievements, are essentially one of the most important indicators

of the development level of agriculture in general.

The leading role among grain crops belongs to wheat and barley. They occupy more than half of the global acreage. This explains the close attention to all issues in one way or another related to the production and harvesting of these crops (Buryanov M. et al., 2015a; Rykov V. et al., 2016; Sokolova E. et al., 2020).

Plants of these crops at the maturation time contain a grain in the ear, which, in natural conditions, in the full ripeness phase gradually loses mechanical connection with it and crumbles in to the field. For the harvest of full-grown grain, it is necessary to carry out timely harvesting before it falls off and artificially force grain separation from the ear (Bello R.S., 2012; Buryanov A. et al., 2015b).

Combine harvesters are now used everywhere for harvesting. Up to now, they are the main machine for crops' harvesting. Their designs implement a method of threshing and primary separation of the harvested heap. This method, invented more than a century ago, involves cutting the entire crop and feeding it into a threshing machine, where it is subjected to the drum beaters impact while being dragged

through a rigid grid. Up to 80% of the power is spent on threshing and grinding the straw, and about 7% of the energy is used to separate the grain from the receptacle.

This impact mode on the processed mass in combines, necessary for the extraction of grain and its separation from the ears of plants through the deck, has serious draw-backs. First, it is energy-consuming. Moreover, secondly, it leads to an overall high level of grain injury up to 20-30% of the entire threshed mass of grain.

Injured grain has reduced germination, and pathogens develop in the resulting cracks during storage. This often makes it impossible to obtain quality seed material, and when a certain level of concentration of microtoxins is reached, the grain is unsuitable not only for the production of baked goods, but also for animal feed.

Moreover, the self-drainage process can occur in grain crops due to insufficient connection of the grain to the ear during untimely harvesting (Buryanov A. et al., 2014). This also causes grain losses, which amount to millions of tons per year.

Thus, pressing issue of the day is to ensure low-energy and low-traumatic forced grain extraction from the ear.

For this purpose, it is necessary not only to improve the existing methods and ways of grain harvesting (Kolesnikov D.A. et al., 2010; Miu P., 2015) but also to develop new highly effective physical-mechanical methods of its harvesting and, accordingly, to design the appropriate equipment (Lachuga U. et al., 2014; Lysenok O. & Matrosov A, 2014; Korotky A. et al., 2019; Ivanov V. et al., 2020). The solution of this problem, on the one hand, requires the development and creation of adequate analytical and numerical physical-mechanical models, including models based on CAD-CAE complexes, which are able to describe the interaction between the elements of the stem-column-grain system. At the same time, on the other hand, there are physical-mechanical models of the process of working bodies of grain harvesting equipment impact on the system stem - spike - grain (Lachuga F. et al., 2019a; Meskhi B. et al., 2019; Pakhomov V. et al., 2020).

## MATERIALS AND METHODS

A block theory can be considered as an approximate mathematical model considering the peculiarities of the geometry. Herewith, in general case, the section characteristics and mechanical properties depend on the longitudinal coordinate of the beam, which leads to boundary value problems with variable coefficients that can be solved analytically only in some particular cases. A simpler model is a beam consisting of two homogeneous parts (stem and spike) in this case the solution could be constructed analytically in both static and harmonic analysis.

### Ear and grain fluctuation mathematical model based on the beam theory

**Continuous one-dimensional ear fluctuation model.** Ear fluctuations are considered within the Euler-Bernoulli beam theory. The ear model is represented by an inhomogeneous beam with variable cross-section, density, and elastic modulus (Figure 1).

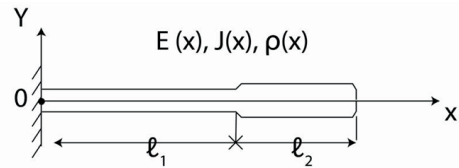


Figure 1. Ear diagram

The lower end of the rod is fixed, a distributed pressure or a concentrated force act on its surface, which in general case depend on time variable, and in special case it is a harmonic influence with circular frequency. The fluctuation equation has the form with respective transverse displacements and appears as following:

$$\frac{\partial^2}{\partial x^2} \left( E(x)J(x) \frac{\partial^2 v}{\partial x^2} \right) + \rho(x) \frac{\partial^2 v}{\partial t^2} = q(x, t) \quad (1)$$

Where:  $E(x)$  - Young's modulus,  $J(x)$  - moment of inertia,  $\rho(x)$  - density.

Boundary conditions:

$$\text{at } x=0 \quad v=0, \quad \frac{\partial v}{\partial x}=0$$

$$\text{at } x = l_1 + l_2, \quad \frac{\partial^2 v}{\partial x^2} = 0, \quad \frac{\partial^3 v}{\partial x^3} = 0 \quad (2)$$

Initial conditions correspond to the absence of motion at the initial moment of time:

$$v(x,0) = 0, \quad \frac{\partial v}{\partial t} \Big|_{t=0} = 0 \quad (3)$$

In general case parameters' dependence of the ear model on the axial coordinate, the solution of the initial boundary value problem 1-3 can be constructed numerically, particular in computer mathematical systems such as Maple or MatLAB mathematical packages, using the built-in numerical integration procedures of differential equations.

According to Figure 1, the rod consists of two main parts, where, in a simplified version, its characteristics can be considered constant. In this case, the mathematical model (4) consists of a differential equations system with constant coefficients and boundary conditions, presented in formula (2), has the following form:

$$E_i J_i \frac{\partial^4 v_i}{\partial x^4} + \rho_i \frac{\partial^2 v_i}{\partial t^2} = q(x,t) \quad i = 1,2 \quad (4)$$

Where:  $E_i$  - Young's modulus,  $J_i$  - moment of inertia,  $\rho_i$  - density, which are constant values at each site.

And the docking equations at:

$$v_1 = v_2, \quad \frac{\partial v_1}{\partial x} = \frac{\partial v_2}{\partial x}$$

$$E_1 J_1 \frac{\partial^2 v_1}{\partial x^2} = E_2 J_2 \frac{\partial^2 v_2}{\partial x^2}, \quad E_1 J_1 \frac{\partial^3 v_1}{\partial x^3} = E_2 J_2 \frac{\partial^3 v_2}{\partial x^3} \quad (5)$$

For harmonic excitation of fluctuations with a circular frequency, the system of equations (4) respecting the amplitude of fluctuations will look like this:

$$E_i J_i \frac{\partial^4 v_i}{\partial x^4} + \rho_i \omega^2 v_i = q(x) \quad (6)$$

The homogeneous ( $q(x) \equiv 0$ ) boundary value equation (6), (2), (5) are considered to find the resonant natural frequencies.

**Relative grain motion equations.** Figure 2 shows the layout of the grain in question and the mobile coordinate system  $O_1 x_1 x_2 x_3$ .

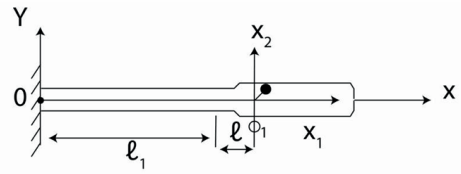


Figure 2. Local (mobile) coordinate system

Figure 3 shows the scheme of grain attachment to the ear, 3 a) - on the stem, 3 b) - without stem. Grain dynamics is investigated in two variants: the first model does not take into account grain size and considers a material point; the second model considers a solid body with a given inertia matrix.

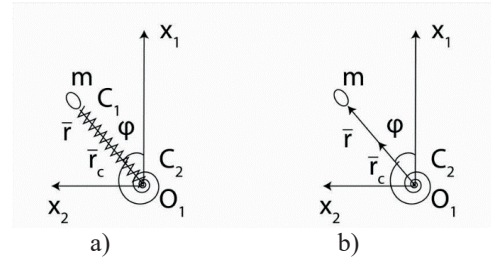


Figure 3. Grain fixing scheme

The linear stiffness spring  $C_1$  and the spiral stiffness spring  $C_2$  simulate grain and ear relationship, moreover the linear spring corresponds to the stem presence and the spiral spring corresponds to the scales interaction.

Choosing a mobile coordinate system coherent with the translational transverse motion of the point ( $x = l_1 + l$ ) of grain to ear attachment, grain acceleration can be represented as follows:

$$\bar{a} = \bar{a}_e + \bar{a}_r \quad (7)$$

Where:  $\bar{a}_e$ ,  $\bar{a}_r$  - transfer acceleration and the relative acceleration, respectively:

$$\bar{a}_e = \left( 0, \frac{\partial^2 v}{\partial t^2} \Big|_{x=l_1+l}, 0 \right) \quad (8)$$

Herewith transport acceleration is found from the solution of the corresponding boundary value problems of Section 2.1.

Then the motion of the grain equation with mass  $m$  in the mobile coordinate system  $O_1 x_1 x_2 x_3$  with initial conditions will take the form:

$$m\ddot{\vec{r}} = \vec{F} - m\vec{a}_e \quad (9)$$

$$\vec{r}|_{t=0} = \vec{r}_c, \quad \dot{\vec{r}}|_{t=0} = 0$$

Where:  $\vec{r} = (x_1, x_2, x_3)$  - radius vector of the grain mass center in motion,  $\vec{r}_c$  - radius vector of the grain mass center before motion commencement,  $\vec{F} = \vec{F}_p + \vec{F}_1 + \vec{F}_2$  the resultant force of the weight and elasticity forces of the linear and circular springs respectively:

$$\vec{F}_p = -(mg, 0, 0), \quad \vec{F}_1 = -C_1 \|\vec{r}\| - |\vec{r}_c| \|\vec{r}\| / |\vec{r}|,$$

$$\vec{F}_2 = \frac{C_2(\varphi - \varphi_0)}{|\vec{r}|} (\sin \varphi, -\cos \varphi, 0), \quad \varphi = \arctan(x_2/x_1) \quad (10)$$

When moving in the plane  $O_1x_1x_2$ , the vector equation (9) is reduced to a system (taking into account the notations  $x_1 = x(t)$ ,  $x_2 = y(t)$ ).

$$\begin{aligned} \frac{d^2}{dt^2}x(t) &= -\frac{C_1| - 1 + \frac{\sqrt{x_0^2 + y_0^2}}{\sqrt{x(t)^2 + y(t)^2}}| x(t)}{m} + \frac{C_2 \left( \arctan\left(\frac{y(t)}{x(t)}\right) - \arctan\left(\frac{y_0}{x_0}\right) \right) y(t)}{\sqrt{x(t)^2 + y(t)^2} x(t) \sqrt{1 + \frac{y(t)^2}{x(t)^2}} m} \\ \frac{d^2}{dt^2}y(t) &= -\frac{C_1| - 1 + \frac{\sqrt{x_0^2 + y_0^2}}{\sqrt{x(t)^2 + y(t)^2}}| y(t)}{m} + \frac{C_2 \left( \arctan\left(\frac{y(t)}{x(t)}\right) - \arctan\left(\frac{y_0}{x_0}\right) \right)}{\sqrt{x(t)^2 + y(t)^2} \sqrt{1 + \frac{y(t)^2}{x(t)^2}} m} + \omega^2 V_0 \sin(\omega t) \quad (11) \end{aligned}$$

Where:  $x_0, y_0$  - initial coordinates of the grain mass center,  $\omega$  - fluctuations' circular frequency of the ear,  $V_0$  - point fluctuations' amplitude  $O_1$  center of grain attachment (Figure 3).

Equations 9 and 10 are nonlinear differential equations and its solutions can be numerically constructed. As a result, maximum elastic force  $F_1$ , moment of elasticity  $M_2 = C_2\varphi$ , and their effect  $A_1, A_2$  in the increasing section  $|\vec{r}|$  and  $|\varphi|$ , can be found

$$A_1 = -C_1 \frac{\|\vec{r}_{\max}\| - |\vec{r}_c|}{2}, \quad A_2 = -C_2 \frac{\varphi_{\max}^2}{2} \quad (12)$$

$$\begin{aligned} y_1(x) &= C_1 \left( \frac{1}{2} \cosh(\beta_1 x) + \frac{1}{2} \cos(\beta_1 x) \right) + C_2 \left( \frac{1}{2} \sin(\beta_1 x) + \frac{1}{2} \sinh(\beta_1 x) \right) \\ &+ C_3 \left( \frac{1}{2} \cosh(\beta_1 x) - \frac{1}{2} \cos(\beta_1 x) \right) + C_4 \left( \frac{1}{2} \sin(\beta_1 x) + \frac{1}{2} \sinh(\beta_1 x) \right) \quad (13) \end{aligned}$$

$$\begin{aligned} y_2(x) &= C_5 \left( \frac{1}{2} \cosh(k\beta_1 x) + \frac{1}{2} \cos(k\beta_1 x) \right) + C_6 \left( \frac{1}{2} \sin(k\beta_1 x) + \frac{1}{2} \sinh(k\beta_1 x) \right) \\ &+ C_7 \left( \frac{1}{2} \cosh(k\beta_1 x) - \frac{1}{2} \cos(k\beta_1 x) \right) \\ &+ C_8 \left( \frac{1}{2} \sin(k\beta_1 x) + \frac{1}{2} \sinh(k\beta_1 x) \right) \quad (14) \end{aligned}$$

In turn these are compared to similar experimental data related to grain extraction from the ear, obtained in experiments on grain extraction from the ear (Shack Yu. et al., 2013; Lachuga Y. et al., 2019b; Matrosov M. et al., 2020).

**Analytical solution to the problem.** The solution of the homogeneous boundary value problem (6), (2), (5) will be found in the form (here and below  $v_1(x), v_2(x)$  denoted by  $y_1(x), y_2(x)$ , a  $l_1, l_2$  and by  $L_1, L_2$  respectively)

where, to simplify the notation, we use the following  $\beta_1 := \frac{p_1 \omega^2}{(E_1 J_1)^{3/4}} L_1$ ,  $k := \frac{p_2 E_1 J_1}{p_1 E_2 J_2} \frac{L_1}{L_2}$   $\cosh(\cdot)$  and  $\sinh(\cdot)$  - are hyperbolic cosine and sine, respectively. The constants  $C_1, C_2, \dots, C_8$  are found further from the boundary and coupling conditions.

Satisfying the boundary conditions at the ends of the beam we obtain

$$C_1 := 0, C_2 := 0, C_7 := 0, C_8 := 0 \quad (15)$$

The docking conditions (5) lead to a linear system:

$$C_3 \left( \frac{1}{2} \cosh(\beta_1 L_1) - \frac{1}{2} \cos(\beta_1 L_1) \right) + C_4 \left( -\frac{1}{2} \sin(\beta_1 L_1) + \frac{1}{2} \sinh(\beta_1 L_1) \right) - C_5 \left( \frac{1}{2} \cosh(k\beta_1 L_2) + \frac{1}{2} \cos(k\beta_1 L_2) \right) - C_6 \left( \frac{1}{2} \sin(k\beta_1 L_2) + \frac{1}{2} \sinh(k\beta_1 L_2) \right) = 0$$

$$C_3 \left( \frac{1}{2} \sinh(\beta_1 L_1) \beta_1 + \frac{1}{2} \sin(\beta_1 L_1) \right) \beta_1 + C_4 \left( -\frac{1}{2} \cos(\beta_1 L_1) \beta_1 + \frac{1}{2} \cos h(\beta_1 L_1) \right) \beta_1 + C_5 \left( \frac{1}{2} \sinh(k\beta_1 L_2) k \beta_1 - \frac{1}{2} \sin(k\beta_1 L_2) k \beta_1 \right) + C_6 \left( \frac{1}{2} \cos(k\beta_1 L_2) k \beta_1 + \frac{1}{2} \cosh(k\beta_1 L_2) \right) k \beta_1 = 0$$

$$C_3 \left( \frac{1}{2} \cosh(\beta_1 L_1) \beta_1^2 + \frac{1}{2} \cos(\beta_1 L_1) \right) \beta_1^2 + C_4 \left( \frac{1}{2} \sin(\beta_1 L_1) \beta_1^2 + \frac{1}{2} \sin h(\beta_1 L_1) \right) \beta_1^2 - C_5 \left( \frac{1}{2} \cosh(k\beta_1 L_2) k^2 \beta_1^2 - \frac{1}{2} \cos(k\beta_1 L_2) k^2 \beta_1^2 \right) - C_6 \left( -\frac{1}{2} \sin(k\beta_1 L_2) k^2 \beta_1^2 + \frac{1}{2} \sinh(k\beta_1 L_2) \right) k^2 \beta_1^2 = 0 \quad (16)$$

$$C_3 \left( \frac{1}{2} \sinh(\beta_1 L_1) \beta_1^3 - \frac{1}{2} \sin(\beta_1 L_1) \right) \beta_1^3 + C_4 \left( \frac{1}{2} \cos(\beta_1 L_1) \beta_1^3 + \frac{1}{2} \cos h(\beta_1 L_1) \right) \beta_1^3 + C_5 \left( \frac{1}{2} \sinh(k\beta_1 L_2) k^3 \beta_1^3 + \frac{1}{2} \sin(k\beta_1 L_2) k^3 \beta_1^3 \right) + C_6 \left( -\frac{1}{2} \cos(k\beta_1 L_2) k^3 \beta_1^3 + \frac{1}{2} \cosh(k\beta_1 L_2) \right) k^3 \beta_1^3 = 0$$

Matrix A of the system (16) looks like:

$$A = \begin{bmatrix} \cosh(\beta_1 L_1) - \cos(\beta_1 L_1) & \sinh(\beta_1 L_1) - \sin(\beta_1 L_1) & -\sin(k\beta_1 L_2) - \sinh(k\beta_1 L_2) & -\cosh(k\beta_1 L_2) - \cos(k\beta_1 L_2) \\ \sinh(\beta_1 L_1) + \sin(\beta_1 L_1) & \cosh(\beta_1 L_1) - \cos(\beta_1 L_1) & k(\cos(k\beta_1 L_2) + \cosh(k\beta_1 L_2)) & k(-\sin(k\beta_1 L_2) + \sinh(k\beta_1 L_2)) \\ \cosh(\beta_1 L_1) + \cos(\beta_1 L_1) & \sinh(\beta_1 L_1) + \sin(\beta_1 L_1) & -k^2(-\sin(k\beta_1 L_2) + \sinh(k\beta_1 L_2)) & k^2(\cos(k\beta_1 L_2) - \cosh(k\beta_1 L_2)) \\ \sinh(\beta_1 L_1) - \sin(\beta_1 L_1) & \cosh(\beta_1 L_1) + \cos(\beta_1 L_1) & -k^3(\cos(k\beta_1 L_2) - \cosh(k\beta_1 L_2)) & k^3(\sinh(k\beta_1 L_2) + \sin(k\beta_1 L_2)) \end{bmatrix}$$

Equality to zero of the determinant  $D = \det(A) = 0$  of the matrix A is the equation aimed at finding natural frequencies.

$$4k(1 - \cosh(\beta_1 L_1) \sin(\beta_1 L_1) k^3 \cosh(k\beta_1 L_2) \sin(k\beta_1 L_2) - \cosh(\beta_1 L_1) \sin(\beta_1 L_1) k^3 \cos(k\beta_1 L_2) \sinh(k\beta_1 L_2) + \cosh(\beta_1 L_1) \cos(\beta_1 L_1) k^4 \cos(k\beta_1 L_2) \cosh(k\beta_1 L_2) + \cos(k\beta_1 L_2) \cosh(k\beta_1 L_2) + \sinh(\beta_1 L_1) \cos(\beta_1 L_1) k \cos(k\beta_1 L_2) \sin h(k\beta_1 L_2) - \sinh(\beta_1 L_1) \cos(\beta_1 L_1) k \cos h(k\beta_1 L_2) \sin(k\beta_1 L_2) - 2 \sinh(\beta_1 L_1) \sin(\beta_1 L_1) k^2 \sin(k\beta_1 L_2) \sinh(k\beta_1 L_2) + \cos(\beta_1 L_1) \sin h(\beta_1 L_1) k^3 \cos h(k\beta_1 L_2) \sinh(k\beta_1 L_2) + k^4 + \cosh(\beta_1 L_1) \cos(\beta_1 L_1) \cos(k\beta_1 L_2) \cosh(k\beta_1 L_2) + \sin(\beta_1 L_1) \cosh(\beta_1 L_1) k \cos(k\beta_1 L_2) \sin h(k\beta_1 L_2) - \sin(\beta_1 L_1) \cos h(\beta_1 L_1) k \cos(k\beta_1 L_2) \sin h(k\beta_1 L_2) + \cosh(\beta_1 L_1) \cos(\beta_1 L_1) - k^4 \cos(k\beta_1 L_2) \cosh(k\beta_1 L_2) - \cosh(\beta_1 L_2) \cos(\beta_1 L_2) k^4 = 0 \quad (17)$$

In particular, with  $k = 0.1$ ,  $L_1 = 0.8 \text{ m}$ ,  $L_2 = 0.09 \text{ m}$ , the dependence of the normalized value of the determinant  $D(\beta_1)$  on the parameter  $\beta_1$  looks like (Figure 4)

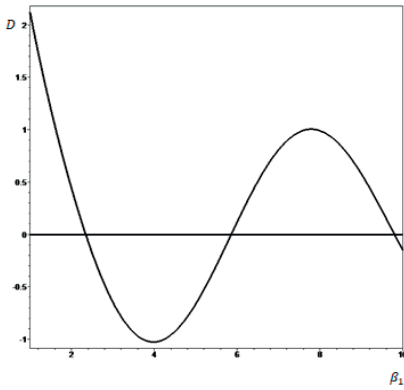


Figure 4. Plot of determinant versus parameter

The first three roots are equal, respectively:

$$\beta_{1_1} = 2.344, \beta_{1_2} = 5.868, \beta_{1_3} = 9.818$$

Analysis of the natural waveforms shows that the form corresponding to the second natural frequency is characterized by intensive movement of the part of the ear containing grains, which agrees with the results obtained earlier by the finite element method. The frequency interval corresponding to the second natural frequency can be called the low-frequency range, in which effective grain extraction from the ear is possible. It should be noted that this mode can be implemented directly in the field when the ear is not separated from the stem and the stem is not cut.

## RESULTS AND DISCUSSIONS

The second frequency range, in which effective grain extraction from the ear is possible, is the range of intense grain vibrations itself in the ear. Here, it should be noted, several modes associated with different grain maturity degrees, namely: the grain is attached to the stalk; the grain is held by the scales. This frequency range can be called - the high-frequency range, because it is a kilohertz interval.

To carry out numerical calculations on the developed mathematical model, experimental data on the deformation and destruction of

plant elements obtained earlier were used (Shack Yu. et al., 2013; Lachuga Y. et al., 2019b; Matrosov M. et al., 2020).

Numerical experiments to determine the grain motion characteristics in this range were carried out in the software complex of finite element analysis ACELAN (Belokon A. et al., 2000; Belokon A. et al., 2002). Quadratic finite elements were used, the finite-element mesh was thickened until the results of the calculations became independent of its shape.

In a numerical experiment the fluctuations of an individual grain at different stages of its maturation were considered: in case of its connection with the ear (early stage) and in the absence of such a connection (late stage).

Modal analysis was carried out, natural resonance frequencies and forms of fluctuations were found. Figures 5-19 show the results for the frequencies at which the fluctuations of the grain contribute to its separation from the ear.

The Figures 5-19 show the parameters of the corresponding value indicated in the figure caption: the blue color corresponds to a smaller value, the red one to a larger one. Figures 5-6 shows the units of measurement. The sides of 1 square are 1 mm. The scale is identical for Figures 5-19.

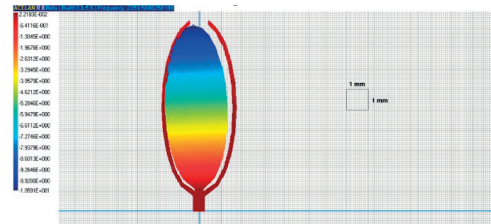


Figure 5. Bending form of grain fluctuation on the stem without scales' connection (horizontal displacement distribution) (fluctuation frequency 2.36 kHz)

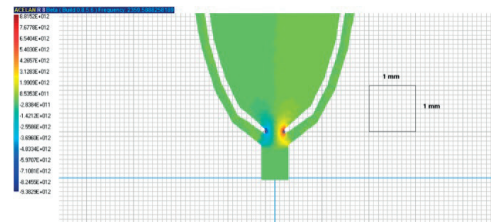


Figure 6. Bending form of grain fluctuation on the stem without scales' connection (distribution of normal vertical stresses) (fluctuation frequency 2.36 kHz)

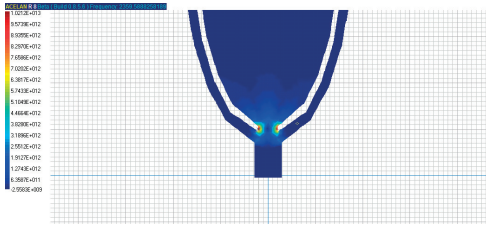


Figure 7. Bending form of grain fluctuations on the stem without scales' connection (stress intensity distribution) (fluctuation frequency 2.36 kHz)

Thus, Figures 5-7 show distributions of the stress-strain state (DSS) of the grain at its own frequency of 2.36 kHz, in the case of its not interacting with the scales, in the presence of connection of the grain with the ear through the stalk. The character of movement corresponds to the fluctuation of the grain at the stalk (Figure 5), in which the maximum stresses arise (Figures 6, 7), this may serve as the basis for its detachment from the ear. Figures 8 and 9 show similar results with a rigid connection between the grain and the flakes, due to their rigidity, the frequency increases compared to the previous case. There is a qualitative overlap of DSS characteristics with the previous case.

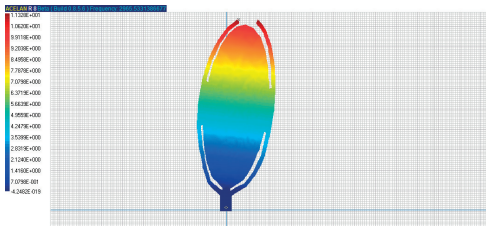


Figure 8. Bending form of grain fluctuation on the stem with a scales' connection (horizontal displacement distribution) (fluctuation frequency 2.97 kHz)

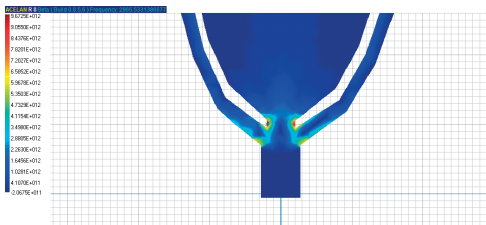


Figure 9. Bending form of grain fluctuation on the stem with scales' connection (stress intensity distribution) (fluctuation frequency 2.97 kHz)

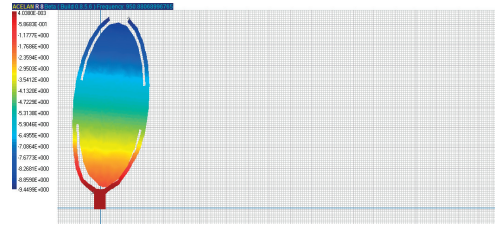


Figure 10. The bending form of grain fluctuation without a stalk with scales' connection (distribution of horizontal displacements) (fluctuation frequency 0.95 kHz)

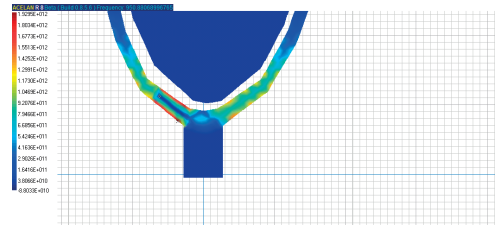


Figure 11. The bending form of grain fluctuations without a stem with scales' connection (stress intensity distribution) (fluctuation frequency 0.95 kHz)

Figures 10 and 11 show the results of bending grain fluctuations in the second maturity stage (no connection with the stalk), the maximum stresses occur at the base of the scales, which may be a sign of their destruction if the fluctuations amplitude is sufficient.

The figures below show fluctuations forms and characteristics of the stress-strain state during vertical movement of the grain without connection with the scales and in the presence of this connection. It should be noted, that the natural sequences in this case are much higher than the previous bending modes.

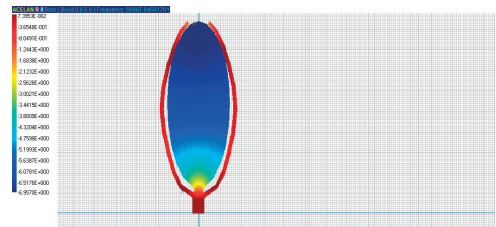


Figure 12. Vertical shape of grain fluctuation on the stem without scales' connection (distribution of vertical displacements) (fluctuation frequency 56.01 kHz)

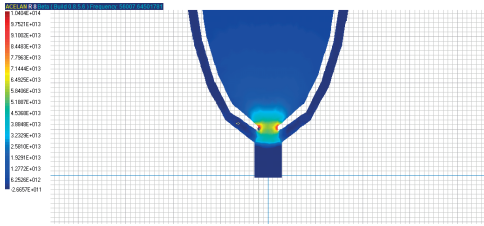


Figure 13. Vertical shape of grain fluctuation on the stem without scales' connection (distribution of stress intensity) (fluctuation frequency 56.01 kHz)

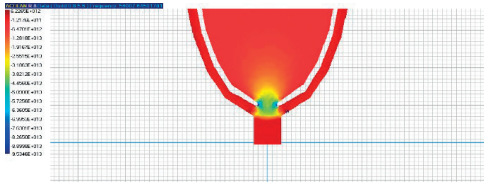


Figure 14. Vertical shape of grain fluctuation on the stem without scales' connection (vertical stress distribution) (fluctuation frequency 56.01 kHz)

Figures 12-14 show the distribution of vertical displacements and voltages at 56.01 kHz in the scale presence. The maximum stress level is in the material of the stalk, which contributes to its destruction. Figures 15-16 show similar results in the presence of a rigid connection to the scales. The natural frequency in this case is slightly lower and is 54.63 kHz. The maximum stress levels also, as in the previous case, occur in the stalk.

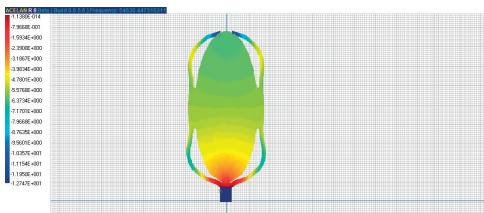


Figure 15. Vertical shape of grain fluctuation on the stem with scales' connection (distribution of vertical displacements) (fluctuation frequency 54.63 kHz)

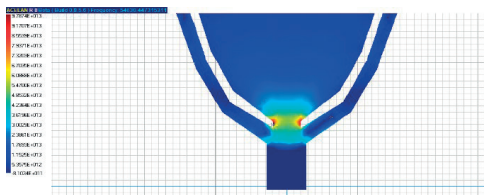


Figure 16. Vertical shape of grain fluctuation on the stem with scales' connection (distribution of stress intensity) (fluctuation frequency 54.63 kHz)

Finally, in this case, at the natural frequency of 61.88 kHz, intensive movement of the grain in the horizontal direction is observed in a fluctuation mode. Figure 17 shows the stress intensity distribution, the maximum of which is observed in the stalk, which contributes to its destruction.

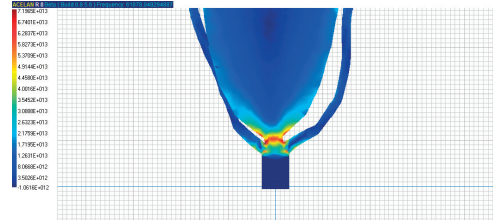


Figure 17. Shape of fluctuations with horizontal shift of the grain on the stem with scales' connection (distribution of stress intensity) (fluctuation frequency 61.88 kHz)

Figures 18-19 show vertical displacements and stress intensity distributions in the absence of the peduncle, but with the grain connection with the scales, at the natural frequency of 11.73 kHz, which, due to the lower rigidity of the scales compared to the peduncle, is much lower than the case in which there is a peduncle. The maximum stresses, as before, occur at the place where the scales are attached to the spike, which will also lead to their detachment.

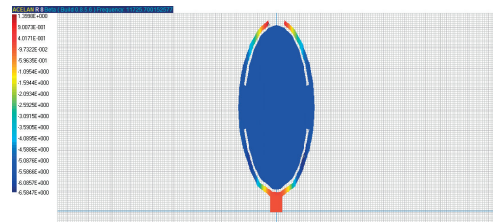


Figure 18. Vertical shape of the fluctuation of the grain without a stem with scales' connection (distribution of vertical displacements) (fluctuation frequency 11.73 kHz)

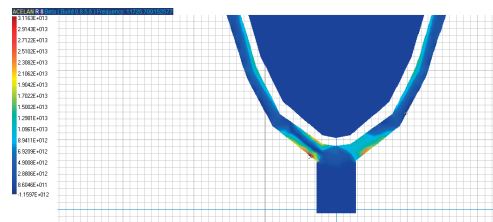


Figure 19. Vertical shape of grain fluctuations without a stem with scales' connection (distribution of stress intensity) (fluctuation frequency 11.73 kHz)

Analysis of the numerical results given in section 3 shows two frequency intervals of effective impact on the plants for the purpose of grain extraction.

The first low-frequency interval (tens of hertz, specific values depend on plant parameters) allows to excite significant ear vibrations, while the stem makes vibrations with relatively small amplitude. This frequency interval of influences can be used under field conditions, which will lead to active grains' extraction from the ear, leaving practically untouched stems.

The second interval is high-frequency (from tenths of kHz to tens of kHz, specific values depend on plant parameters and degree of grain ripening) characterized by intensive grain movement: these are bending grain movements with the stem and scales, which can lead to separation of the grain through breaking scales from the ear; and grain movement along the chamber, which can lead to its separation leaving scales undamaged, which is most beneficial from an energy consumption perspective.

## CONCLUSIONS

The article presents developed series of fluctuation models of the stem with the ear and the individual grain in the ear. The applied beam theory and the general continuum formulation within the linear theory of elasticity are used. Numerical calculations on the basis of the general model by means of the finite element method were performed. Numerical calculations of natural frequencies, fluctuation forms, and established fluctuations of the developed approaches are carried out both for the plant as a whole and its parts separately. The developed applied theories have shown their adequacy within the limits of their applicability.

Thus, models and tools for vibration analysis have been developed, allowing finding vibration amplitudes, mechanical stresses or forces (forces and moments) both analytically or numerically. These can be compared to critical values in plant elements destruction and grain extraction.

The natural frequencies show that at the value of natural frequencies of grain fluctuations

131,6 Hz and 1274,9 Hz the grain itself fluctuates predominantly, and at frequencies 1622,8 Hz, 7367.3 Hz, 9396.0 Hz and 13491,0 Hz the flakes vibrate.

Earlier field tests confirmed the results of theoretical and numerical analysis on the presence of two impact frequency ranges on the plant as a whole and on the ear, at which grains can be effectively extracted from the ear.

## FUNDING

This research was funded by Don State Technical University.

## ACKNOWLEDGMENTS

This work was carried out within the framework of the Presidential grant of the Russian Federation for state support of young Russian scientists (MK-1700.2021.5, agreement №075-15-2021-179).

## REFERENCES

- Andruszczak, P.K.S., Dziki, D., Stocki, M., Stocka, N., Paweł, K.R. (2019). Gierasimiuk. "Green Grain of Spelt (Triticum aestivum ssp. Spelta) Harvested at the Stage of Milk-Dough As a Rich Source of Valuable Nutrients". *Emirates Journal of Food and Agriculture*, 31, doi:<https://doi.org/10.9755/ejfa.2019.v31.i4.1931>.
- Bayin, S.S. (2019). *Essentials of Mathematical Methods in Science and Engineering*, Publisher: John Wiley & Sons Inc., Turkey, pp 960.
- Bello, R.S. (2012). *Agricultural Machinery & Mechanization*, Publisher: Dominion Services, Nigeria, 2012; p. 355.
- Belokon, A., Ereneyev, V., Nasedkin, A., Solovyev, A. (2000). Partitioned schemes of the finite-element method for dynamic problems of acoustoelectroelasticity. *Journal of Applied Mathematics and Mechanics*, 64, 3, P. 367-377. DOI 10.1016/S0021-8928(00)00059-9.
- Belokon, A., Nasedkin, A., Solovyev, A. (2002). New schemes for the finite-element dynamic analysis of piezoelectric devices. *Journal of Applied Mathematics and Mechanics*, 66, 3, P. 481-490. DOI 10.1016/S0021-8928(02)00058-8.
- Berihuete-Azorin, M., Stika, H-P., Hallama, M., Valamoti, S. M. (2020). Distinguishing ripe spelt from processed green spelt (Grünkern) grains: Methodological aspects and the case of early La Tène Hochdorf (Vaihingen a.d. Enz, Germany), *Jour. of Arch. Sci.*, 118, 105143, 0305-4403. <https://doi.org/10.1016/j.jas.2020.105143>
- Buryanov, A., Kostylenko, O. (2014). On the dynamics of winter wheat grain shedding under weather

- conditions in 2013. *In Development of innovative technologies and technical means for the agro-industrial complex: Collection of scientific papers of the 9th International Scientific practical conference in 2 parts*, pp. 121-128.
- Buryanov, M., Buryanov, A., Chervyakov, I. (2015a). Methods of mathematical modeling of the process of grain movement in the transporting channel of the stripping header. *Tractors and agricultural machines*, 10, 27-30.
- Buryanov, A., Buryanov, M., Goryachev, Yu., Kostylenko, O. (2015b). The effect of the grain loss value by harvesting machines on their efficiency, *In State and prospects of agricultural engineering development: collection of scientific works of the 8th international scientific-practical conference*, p. 19-22
- Huang, T., Li, B., Shen, D., Cao, J., Mao, B. (2017). Analysis of the grain loss in harvest based on logistic regression. *Proc. Comp. Sci.*, 122, 698-705 <https://doi.org/10.1016/j.procs.2017.11.426>
- Ivanov, Yu., Pakhomov, V., Kambulov, S., Rudoy, D. (2018). Determination of the parameters of the hydrodynamic mixer. *MATEC Web of Conf.*, 05023 <https://doi.org/10.1051/mateconf/201822405023>
- Ivanov, V., Popov, S., Dontsov, N., Ekinil, G., Oleynikova, Ju. (2020). Denisenko Ju. Mechanical coating formed under conditions of vibration exposure. *E3S Web of Conf.*, 175, 05023 [doi.org/10.1051/e3sconf/202017505023](https://doi.org/10.1051/e3sconf/202017505023).
- Kolesnikov, D.A., Matrosov, A.A. (2010). Calculation of strength characteristics and service life of the rear axle of the combine. State and prospects for the development of agricultural engineering. *Materials of the 3rd international. scientific-practical Conf.*, 200-202
- Korotky, A., Marchenko, E., Ivanov, V., Popov, S., Marchenko, Ju., Dontsov, N. (2019). Model of forming vibration mechanochemical solid lubrication coating on surface of steel rope. *In XII International Scientific Conference on Agricultural Machinery Industry (INTERAGROMASH, 2019): IOP Conference Series: Earth and Environmental Science*, pp. 012116. doi:10.1088/1755-1315/403/1/012116.
- Korotun, A.A., Matrosov, A.A. (2010). Calculation of strength characteristics and service life of the combine frame State and prospects for the development of agricultural engineering. *Proceedings of the 3rd international. scientific-practical Conf.*, 217
- Lachuga, U., Pakhomov, V., Buryanov, A. (2013). Ocher: technology, technique, prospects, *In Innovative technologies in science and education. ITNO-2013: collection of scientific works of scientific and methodical conference*, pp. 47-51.
- Lachuga, F., Matrosov, A., Panfilov, I., Pakhomov, V., Rudoy, D. (2019a). Mathematical model of wheat ear dynamics. *Mathematical modeling and biomechanics in modern university*, pp 91
- Lachuga, Y., Soloviev, A., Matrosov, A., Panfilov, I., Pakhomov, V., Rudoy, D. (2019b). Analytical model of ear dynamics and conditions for efficient grain extraction. *IOP Conf. Series: Earth and Environmental Science*, 403, 012055 doi:10.1088/1755-1315/403/1/012055
- Lachuga, Y., Alabushev, A., Pakhomov, V., Ionova, E., Khlystunov, V. (2019c). Physico-mechanical characteristics of connections and biological features of separating grain from ear. *IOP Conf. Ser.: Earth Environ. Sci.*, 403 012050
- Lysenok, O., Matrosov, A. (2014). Evaluation of the efficiency of the comb of the conveyor of the feeder chamber of the combine. *In State and prospects for the development of agricultural engineering: Proceedings of the 7th international. scientific-practical Conf.*, pp. 86-87.
- Matrosov, M., Nizhnik, D., Panfilov, I., Pakhomov, V., Serebryanaya, I., Soloviev, A., Rudoy, D. (2020). Calculation of the movement trajectory of the grain mass in the field stripper. *E3S Web of Conf.*, 210, 08015 <https://doi.org/10.1051/e3sconf/202021008015>
- Menter, F.R., Egorov, Y. (2010). The Scale-Adaptive Simulation Method for Unsteady Turbulent Flow Predictions. Pt. 1: Theory and Model Description. *Journal Flow Turbulence and Combustion*, 85, 113-138
- Meskhii, B., Pakhomov, V., Rudoy, D., Butovchenko, A., Soloviev, A., Olshevskaya, A., Doroshenko, A. (2019). Organizational and technological design bases in agricultural production, Publisher: DSTU, Russia, Rostov-on-Don. P. 548.
- Miu, P. (2015). Combine Harvesters: Theory, Modeling, and Design. *CRC Press Taylor and Francis*, DOI: 10.1201/b18852.
- Özkaya, B., Turksöy, S., Özkaya, H., Baumgartner, B., Özkeser, İ., Köksel, H. (2018). Changes in the functional constituents and phytic acid contents of firiks produced from wheats at different maturation stages. *Food Chemistry*, 246, 150-155 doi: 10.1016/j.foodchem.2017.11.022
- Pakhomov, V., Rykov, V., Kambulov, S., Shevchenko, N., Revyakin, E. (2015). Experience of Winter Wheat Cultivation in Insufficient Moisture Conditions. *Moscow: Rosinformagrotech*, 160
- Pakhomov, V., Rykov, V., Kambulov, S., Kambulov, I., Demina, E., Kolesnik, V. (2016). Grain quality of winter wheat depending on cultivation technologies. *Russian Grain Farming*, 6, 55-59.
- Pakhomov, V., Braginet, S., Bakhchevnikov, O., Rudoy, D., Chernutsky, M.V. (2020). Research results of vibration extraction of grain from the ear possibility of. *Polythème Network Electronic Scientific Journal of Kuban State Agrarian University*, 155. pp 25-42.
- Pinder, G.F. (2018). Numerical Methods for Solving Partial Differential Equations, A Comprehensive Introduction for Scientists and Engineers, Publisher: Wiley, USA, pp. 309.
- Risius, H., Prochnow, A., Ammon, C., Mellmann, J., Hoffmann, T. (2017). Appropriateness of on-combine moisture measurement for the management of harvesting and postharvest operations and capacity planning in grain harvest. *Bio. Eng.*, 156, 120-135, 1537-5110, <https://doi.org/10.1016/j.biosystemseng.2017.01.012>.

- Rybas, I., Gureeva, A. (2016). Winter soft wheat spike productivity in the southern part of the Rostov region in the ecological plasticity indicators. *International Scientific and Research Journal*, 5 (47), 6, 52-56.
- Rykov, V., Kambulov, S., Kambulov, I., Kolesnik, V., Demina, E., Ridnyi, S. (2016). Cultivation technologies effect on winter wheat grain toxicity indicators. *Science in Central Russia*, 6(24), 36-42.
- Shack, Yu., Pakhomov, V., Buryanov, A. (2013). Analytical model of ear dynamics and conditions for efficient grain extraction. *Innovative technologies in science and education ITNO-2013*, pp 47-51
- Sokolova, E., Orobets, V., Sevostyanova, O., Gorchakov, E., Rudoy, D., Olshevskaya, A., Babajanyan, A. (2020). Toxicological evaluation of a new iron-containing preparation for farm animals with alimentary anemia. *E3S Web of Conferences*, 175, 03015, <https://doi.org/10.1051/e3sconf/202017503015>.
- Soloviev, A., Matrosov, A., Panfilov, I., Meskhi, B., Polushkin, O., Rudoy, D., Chebanenko, V. (2020). Mathematical and laboratory modeling of resonant impact on the spike for the purpose of grain selection. *E3S Web of Conf.*, 210, 05017 <https://doi.org/10.1051/e3sconf/202021005017>
- Yu, H., Li, B., Shen, D., Cao, J., Mao, B. (2017). Study on prediction model of grain post-harvest loss. *Proc. Comp. Sci.*, 122, 122-129, 1877-0509 <https://doi.org/10.1016/j.procs.2017.11.350>.
- Ziborov, E.N., Matrosov, A.A. (2010). Calculation of strength characteristics and service life of the front axle of a combine State and prospects for the development of agricultural engineering. *Proceedings of the 3rd international. scientific-practical Conf.*, 199-200